

Broadband absorption and *ab initio* results on the CF $C^2\Sigma^+ - X^2\Pi$ system

Jorge Luque^{a)} and Eric A. Hudson
Lam Research Corporation, Fremont, California 94538

Jean-Paul Booth
Laboratoire de Physique et Technologie des Plasmas, Ecole Polytechnique, 91128 Palaiseau, France

Ioannis D. Petsalakis
Theoretical and Physical Chemistry Institute, The National Hellenic Research Foundation,
48 Vassileos Constantinou Avenue, Athens 11635, Greece

(Received 3 July 2002; accepted 14 October 2002)

Broadband absorption spectra and *ab initio* calculations are combined to complete and reinterpret part of the vacuum ultraviolet spectra of the CF radical. We have found a new band at 190.8 nm which we have assigned to the CF $C^2\Sigma^+ - X^2\Pi$ (1,0) transition. *Ab initio* calculations show that the band at 186.6 nm formerly assigned as CF $C'^2\Sigma^+ - X^2\Pi$ (0,0) by White *et al.* [J. Mol. Spectrosc. **75**, 318 (1979)] corresponds to the CF $C^2\Sigma^+ - X^2\Pi$ (2,0) band. The CF $C^2\Sigma^+$ state is heavily perturbed by the $A^2\Sigma^+$ state and by repulsive $^2\Sigma^+$ states. The observed predissociation pattern for the $C^2\Sigma^+$ ($v'=0,1,2$) states is well reproduced by the calculations. Information on the CF $C^2\Sigma^+ - X^2\Pi$ and $D^2\Pi - X^2\Pi$ electronic transition moments and corresponding oscillator band strengths is also presented. © 2003 American Institute of Physics. [DOI: 10.1063/1.1526637]

I. INTRODUCTION

The CF radical is a common intermediate in fluorocarbon chemistry in either plasmas¹⁻⁴ or flames.⁵ Ultraviolet spectroscopy is one of the most extended methods to obtain information on the CF radical in hostile environments.^{2,6-9} The $A^2\Sigma^+ - X^2\Pi$ and $B^2\Delta - X^2\Pi$ bands have been the subject of many studies because they are located between 195 and 235 nm, where experimental work is easily accessible. Two-photon excitation processes on the CF $D^2\Pi - X^2\Pi$ bands¹⁰⁻¹² have facilitated the study of part of the vacuum ultraviolet. Johnson and Hudgens¹⁰ mention that no other bands are observed in the CF $D^2\Pi - X^2\Pi$ spectral region, even though transitions to the $C(2^2\Sigma^+)$ and $C'^2\Sigma^+$ states, identified by White *et al.*,^{13,14} should be detectable. They explain the lack of additional spectral features in the two-photon spectra by the fast predissociation of the $C^2\Sigma^+$ and $C'^2\Sigma^+$ states.

There has only been one extensive study to date on the vacuum ultraviolet transitions of the CF radical by White,¹⁴ which has only been partially published.^{13,15} A common characteristic of the spectral transitions observed in the vacuum UV spectra of the CF radical is the existence of extensive perturbations and predissociation. White's experimental study was accompanied by theoretical calculations^{13,15} to help assign bands to different electronic transitions. Relevant to this work was the assignment of the band at 195 nm to the $C^2\Sigma^+ - X^2\Pi$ (0,0) transition, the 186.6 nm band to $C'^2\Sigma^+ - X^2\Pi$ (0,0), and the 191.2 nm band to $C' - X$ (0,1). White *et al.*^{13,14} correlated the $C^2\Sigma^+$ state to the $3p\sigma$ ($2^2\Sigma^+$) Rydberg state and suggested the $C'^2\Sigma^+$

$v'=0$ state could be a perturbed vibrational level of the $A^2\Sigma^+$ state because they could not find a state in their calculations at the right energy to correlate with the observations. Recently, Petsalakis¹⁶ found a similar problem trying to assign the $C'^2\Sigma^+ - X^2\Pi$ (0,0) transition to the excited states predicted by his calculations.

In the present paper we have analyzed the absorption spectrum of the CF radical between 189 and 202 nm. Besides the $B^2\Delta - X^2\Pi$ (0-2,0) bands, we have identified the $C^2\Sigma^+ - X^2\Pi$ (1,0), (0,0), (2,1), and (0,1) bands. The $C^2\Sigma^+ - X^2\Pi$ (1,0) and (0,0) bands are broadened by predissociation, and their intensity in absorption is comparable to those of the $A^2\Sigma^+ - X^2\Pi$ and $B^2\Delta - X^2\Pi$ bands. We have employed the complex coordinate method and previously calculated published and unpublished *ab initio* data by Petsalakis¹⁶ to predict energy terms, and predissociation of the $C^2\Sigma^+$ state. The agreement is remarkably good for $C^2\Sigma^+$ $v'=0,1$ and suggests that the $C'^2\Sigma^+$ $v'=0$ state assigned by White is in fact the $C^2\Sigma^+$ $v'=2$ state. This resolves one of the remaining problems in the vacuum UV spectral assignment of the CF radical.

II. BROADBAND ABSORPTION EXPERIMENTAL DETAILS

The experimental method is described in more detail in a recent paper on the CF $A^2\Sigma^+ - X^2\Pi$ and $B^2\Delta - X^2\Pi$ bands.¹⁷ In brief, radical species were generated in an Exelan[®] High Performance (Lam Research Corp.) dielectric etch system. This is a dual-frequency (2 MHz, 27 MHz), capacitively coupled commercial etch system, designed for wafer processing and equipped with fused silica viewports on opposite sides of the chamber. Radical species were gen-

^{a)}Electronic mail: Jorge.Luque@lamrc.com

erated using a combination of argon and cyclooctafluorobutane ($c\text{-C}_4\text{F}_8$) feed gases at a pressure of 160 mTorr and total rf powers of 2 kW in both rf sources.

The UV source was a Xenon arc lamp (Oriel, 150 W) equipped with an $f/1.5$ collimating lens and a shutter. UV-enhanced aluminum mirrors (Thorlabs, Inc.) were used to direct the exit beam to a condensing lens (Edmund Scientific Co.), which focused the beam onto the entrance slit of a spectrograph (SP-750i, Acton Research Corp., 0.75 m Czerny-Turner). The spectra were taken with a 2400 l/mm grating and typical spectral resolution is 0.02 nm. The wavelength scale was calibrated with suitable atomic transitions in the range of 193–260 nm. The accuracy was 4 cm^{-1} (~ 1 pixel) for the 2400 l/mm grating including the error in grating position reproducibility. The light detector was a 1024-channel photodiode array (DM-220, Andor Technology Corp.), and its linearity was calibrated in the range used for spectral measurements.

Absorption spectra were measured by combining four separate measurements, taken under different conditions: detector background (plasma off, shutter closed); source (plasma off, shutter open); full spectrum (plasma on, shutter open); and optical emission (plasma on, shutter closed). The last measurement is required to remove the contribution of optical emission from excited species in the plasma, which can be considerable for some plasma species. Stray light might become a source of systematic error when it is more than a few percent of the total light spectral irradiance. It decreases the true absorbance value by the percentage of stray light in the lamp spectrum. This situation is likely with measurements near the O_2 absorption onset at 195 nm. The stray light was estimated by the difference between the transmitted light in the optically dense spectral region below 190 nm and the detector background spectra.

The absorbance (A) spectra were calculated as follows:

$$\ln \frac{I_{\text{source+plasma}} - I_{\text{plasma emission}}}{I_{\text{source}} - I_{\text{background}}} = -A = -n\sigma L \quad (1)$$

and interpreted by the Lambert–Beer law, where n is the average number density in the optical path (cm^{-3}), σ is the absorption cross section (cm^2), and L is the optical path length where the absorbers are distributed. Integrating the absorbance in frequency for a spectral transition and with $n\sigma L \ll 1$,

$$\int \frac{I_0 - I(\nu)}{I_0} d\nu = \pi r_e f_{\nu', \nu''} n L, \quad (2)$$

where I_0 is the light beam initial intensity, $I(\nu)$ is the intensity after passing the sample, r_e is classical radius of the electron, ν is the frequency (cm^{-1}), and $f_{\nu', \nu''}$ is the oscillator strength of the transition between two vibrational levels.

Spectral computer simulation of the rotational structure of the different vibronic transitions was used to identify bands, estimate line shape broadening, determine band overlaps, and measure temperatures. The database/spectral simulation program LIFBASE¹⁸ was modified to include the CF $A^2\Sigma^+ - X^2\Pi$, $B^2\Delta - X^2\Pi$, $C^2\Sigma^+ - X^2\Pi$ and $D^2\Pi - X^2\Pi$ bands. Line shape and population distributions are selectable parameters to model the spectra. Absolute transition prob-

abilities from calculations in the present study are included in the database. We note that the only elements from *ab initio* calculations in the spectral simulation are the electronic transition moments. The other factors in the spectral simulations, including the band positions, rotational constants, Franck–Condon factors, and predissociation rates are from spectroscopic analysis of the data in the present paper or from other experiments.¹⁴

III. AB INITIO CALCULATIONS

The details of the *ab initio* calculations used to derive potential energy curves, transition strengths, and predissociation rates have been reported previously by Petsalakis.¹⁶ For the purpose of the present work, in addition to the calculated potential energy curves, rotational electronic and radial matrix elements reported earlier, the $C^2\Sigma^+ - X^2\Pi$, $C^2\Sigma^+ - A^2\Sigma^+$, $D^2\Pi - X^2\Pi$, and $D^2\Pi - A^2\Sigma^+$ electronic dipole transition moments were calculated for values of internuclear distance between 0.9 and 2.4 Å. Furthermore, the potential energy curve of the $1^4\Sigma^-$ state was added to complete the picture of the lower lying states of CF. Predissociation widths of the first seven vibrational levels of the $C^2\Sigma^+$ state for rotational levels $N=0, 5, 10, 15, 20, 25$, and 30 were calculated using a five-state coordinate calculation similar to the previous calculations for the $\nu'=0$ level of this state.¹⁶ These additional calculations were necessary for the interpretation of the observed spectra.

IV. RESULTS AND DISCUSSION

A. Ab initio calculations

The *ab initio* potential curves of the lower lying states of CF are shown in Fig. 1. The $A^2\Sigma^+$, $C^2\Sigma^+$, and $D^2\Pi$ Rydberg states and the $B^2\Delta$ valence states show complicated shapes, which result from their mutual interactions and avoided crossings. The $D^2\Pi$ state has a characteristic Rydberg shape at short internuclear distance; at 1.5 Å it has a maximum from an avoided crossing with repulsive valence states. The $A^2\Sigma^+$ and $C^2\Sigma^+$ Rydberg states change character at long distances as indicated by the avoided crossings. Finally, the $B^2\Delta$ state shows a maximum at 1.9 Å as a result of an avoided crossing with a repulsive $^2\Delta$ state correlating with ground state dissociation limits. The agreement between the vertical calculated transition energies and experimental values is within 0.1 eV for the four states while for the $C^2\Sigma^+$ state the error is only 0.03 eV (cf. Table II of Ref. 16). Table I shows the vibrational spacing and rotational constants obtained from the $C^2\Sigma^+$ state potential curve. The rotational constants and vibrational spacings are much smaller than those expected from an unperturbed Rydberg state. Vibrational spacing and rotational constants do not decrease steadily as expected with vibrational level, further confirming the complex interactions of the $C^2\Sigma^+$ state with other states, mainly by the avoided crossing with the $A^2\Sigma^+$ state. Early calculations using the multiconfiguration Hartree–Fock method¹³ found this state to be very similar to the $A^2\Sigma^+$ Rydberg state with comparable potential curve parameters ($B_e = 1.719\text{ cm}^{-1}$, $\alpha_e = 0.0186\text{ cm}^{-1}$, $\omega_e = 1846$

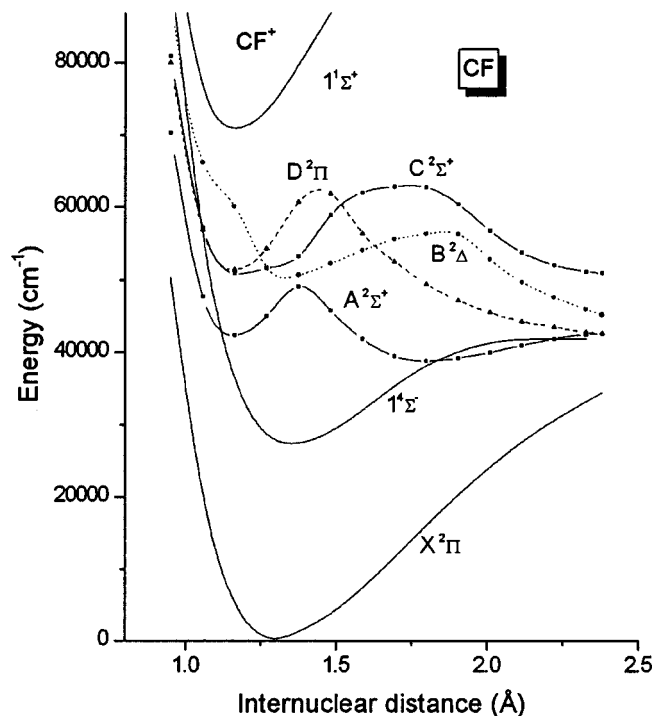


FIG. 1. Potential energy curves of the $X^2\Pi$, $A^2\Sigma^+$, $B^2\Delta$, $C^2\Sigma^+$, $D^2\Pi$ states of CF. The quartet $1^4\Sigma^-$ and the singlet ground state of CF^+ are also shown.

cm^{-1} , $\omega_e x_e = 22.9\text{ cm}^{-1}$). However, this method is known to be inaccurate for treating complex interactions and for predicting avoided crossings.

Figure 2 and Table II show the electronic transition moment for the $C-X$, $C-A$, $D-X$, and $D-A$ transitions. The $C-X$ transition dipole moment has a smooth shape with a maximum at 1.45 Å coinciding with the change of Rydberg character in the $C^2\Sigma^+$ state. Also the rotational-electronic interaction switches from $C-D$ to $C-X$ dominated at this distance (Fig. 7 in Ref. 16). The $C-A$ transition is very strong at short internuclear distances. The sharp change between 1.2 and 1.5 Å is coincidental with the sharp maximum in the radial coupling between the $C^2\Sigma^+$ and $A^2\Sigma^+$ states (Fig. 6 in Ref. 16).

The potential energy curves, radial coupling interactions, and rotational-electronic interactions are included in a mul-

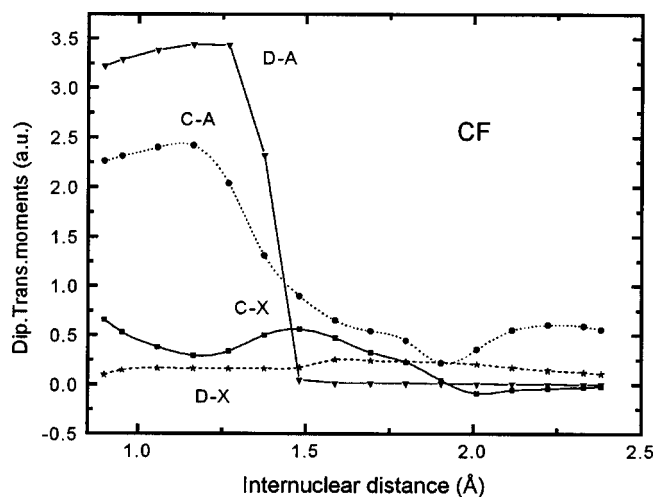


FIG. 2. Calculated dipole transition electronic moments for the $C^2\Sigma^+ - X^2\Pi$, $C^2\Sigma^+ - A^2\Sigma^+$, $D^2\Pi - X^2\Pi$, and $D^2\Pi - A^2\Sigma^+$ transitions of the CF radical.

tistate complex coordinate rotation calculation of vibrational rotational levels and their widths. Results for the $C^2\Sigma^+$ state are given in Table III. The $C^2\Sigma^+$ state is strongly predissociated. In general, predissociation increases with vibrational level and is nearly independent of the rotational quantum number. The exception is the $v'=2$ vibrational level that is very weakly predissociated at low rotational quantum numbers. The main mechanism for predissociation is the strong radial interaction with the $A^2\Sigma^+$ state, consistent with the low rotational dependence of predissociation. The $C^2\Sigma^+$ state also has strong rotational-electronic coupling with the $D^2\Pi$ and the ground state $X^2\Pi$. The effects of the various interactions cancel out a large part of the radial coupling for $C^2\Sigma^+ v'=2$, leaving rotational-electronic coupling as dominant for large rotational quantum number values.

B. Absorption spectra

Figure 3 shows the absorption spectrum of the CF radical in the region between 188.5 and 201 nm . There are assignable bands from the CF $B-X$ system at 194 and 198 nm that correspond to the $B-X(2,0)$ and $(1,0)$ bands respectively. The band at 194.7 nm was assigned by White *et al.* as

TABLE I. Summary containing the experimental and calculated vibrational spacings, rotational constants, and predissociation lifetimes of the CF $C^2\Sigma^+$ state. Calculated predissociation lifetimes are given for rotational quantum number $N=10$.

$C^2\Sigma^+$ v'	Vibrational spacing (cm^{-1})		Predissociation lifetime (ps)		$B_{v'}$ (cm^{-1})	
	Calculated	Observed	Calculated	Observed	Calculated	Observed
0			1.70	1.3 ± 0.4	1.564	1.595 ± 0.007^a
1	1111	1135	0.43	0.5 ± 0.1	1.490	~ 1.56
2	1090	1181	500	$\sim 10.0^a$	1.485	1.5327 ± 0.0006^a
3	1273		0.21		1.495	
4	1351		0.05		1.496	
5	1352		0.02		1.450	
6	1284		0.01		1.432	

^aFrom White *et al.* (Refs. 13 and 14).

TABLE II. *Ab initio* electronic transition moment in atomic units (1 D=0.3935 a.u.) for the CF $C^2\Sigma^+-X^2\Pi$, $C^2\Sigma^+-A^2\Sigma^+$, $D^2\Pi-X^2\Pi$, and $D^2\Pi-A^2\Sigma^+$ systems. The $C^2\Sigma^+-X^2\Pi$ transition moment has to be increased by 25% to match the relative intensities of the CF $B-X(0,0)$ and (1,0) bands of the spectrum in Fig. 3.

Internuclear distance in Å (bohr in parentheses)	$C^2\Sigma^+-X^2\Pi$	$C^2\Sigma^+-A^2\Sigma^+$	$D^2\Pi-X^2\Pi$	$D^2\Pi-A^2\Sigma^+$
0.900 (1.7)	0.657 230	2.308 750	0.100 718	3.219 330
0.953 (1.8)	0.530 060	2.396 350	0.146 551	3.289 520
1.058 (2.0)	0.380 230	2.418 220	1.167 129	3.385 600
1.164 (2.2)	0.295 140	2.031 820	0.165 129	3.440 650
1.270 (2.4)	0.340 100	2.031 820	0.160 507	3.435 650
1.375 (2.6)	0.499 040	1.306 710	0.161 740	2.323 600
1.481 (2.8)	0.558 060	0.897 870	0.173 335	0.048 129
1.587 (3.0)	0.470 310	0.649 430	0.252 161	0.013 508
1.693 (3.2)	0.327 010	0.541 880	0.243 220	0.013 569
1.799 (3.4)	0.228 520	0.444 310	0.236 429	0.012 708
1.904 (3.6)	0.044 160	0.217 510	0.224 940	0.011 943
2.010 (3.8)	-0.088 580	0.356 690	0.207 074	0.009 424
2.116 (4.0)	-0.055 690	0.548 390	0.173 050	0.006 719
2.222 (4.2)	-0.039 920	0.602 870	0.144 073	0.003 566
2.328 (4.4)	-0.026 510	0.590 700	0.124 145	0.000 854
2.381 (4.5)	-0.020 840	0.552 980	0.109 846	0.000 136

CF $C-X(0,0)$, but the peaks at 190.7 and 199.7 nm have not been reported to date. We assign them as the CF $C-X(1,0)$ and (0,1) bands. The shoulder overlapping the $C-X(1,0)$ band at 191.2 nm corresponds to the $C'-X(0,1)$ band as assigned by White *et al.* and which we reassign as the $C-X(2,1)$ band. The signal-to-noise ratio decreases quickly toward 190 nm because of the O_2 interference in the optical pathway. Figure 3 shows the assignment of the O_2 $B^3\Sigma_u^- - X^3\Sigma_g^-$ Schumann-Runge bandheads,¹⁹ which grow quickly in intensity toward the vacuum UV, blocking the xenon lamp light below 188 nm. Degradation in the quality of the absorption spectra is caused by the O_2 $B-X(3,0)$, (4,0) and (5,0) bands. The incomplete removal of the O_2 absorbance in the optical path produces negative and positive spikes on top of the CF spectral features. The $C-X(0,0)$ band is mildly effected by the O_2 $B-X(3,0)$ band, whereas the O_2 $B-X(4,0)$ band is clear at 192.5 nm.

Finally, the O_2 $B-X(5,0)$ has an even larger effect. We have removed the obvious spikes in the $C-X(1,0)$ band to facilitate the comparison with simulation.

The experimental spectral resolution is 0.02 nm or ~ 5 cm^{-1} , but the $C-X(0,0)$ and especially the $C-X(1,0)$ band appear broadened. White *et al.* already mentioned that the $C-X(0,0)$ band is diffuse, so they only analyzed the band-head positions to obtain a rotational constant of 1.60 cm^{-1} . The CF $D-X(0,0)$ transition is known to be at 190.4 nm, but it is not observed in Fig. 1. Three factors contribute to the lack of absorption from $D-X(0,0)$. First, it overlaps with the strong $C-X(1,0)$ band. Second, it also overlaps with the O_2 $B-X(5,0)$ bandhead. Finally, the transition is weak; White observed the $D-X(2,0)$ and (1,0) bands, but not the fundamental (0,0). The CF $C-X(1,0)$ transition was not reported by White¹⁴ either. Perhaps the broadened band appeared as an absorption background in their photographic plates. Re-

TABLE III. Calculated energies in cm^{-1} (referred to $C v'=0, N'=0$) and predissociation lifetimes for the first seven vibrational levels of the $C^2\Sigma^+$ electronic state of CF for selected rotational levels.

N	v	v						
		0	1	2	3	4	5	6
0	E	0	1111.0	2201.3	3474.3	4825.1	6178.2	7462.8
	τ	1.7ps	0.43ps	97.4 ns	0.22ps	0.05ps	0.02ps	0.01ps
5	E	44.1	1152.9	2243	3516.2	4867.1	6219.2	7502.7
	τ	1.7ps	0.43ps	10.9 ns	0.21ps	0.05ps	0.20ps	0.01ps
10	E	169.9	1272.3	2362.2	3636.3	4986.7	6336	7617.1
	τ	1.7ps	0.43ps	0.52ns	0.21ps	0.05ps	0.02ps	0.01ps
15	E	374.2	1466.1	2555.6	3830.9	5180.9	6525.2	7802.3
	τ	1.6ps	0.44ps	0.10ns	0.20ps	0.05ps	0.02ps	0.01ps
20	E	656.4	1734.1	2823.1	4100.4	5449.6	6786.4	8058.7
	τ	1.5ps	0.45ps	32.0 ps	0.18ps	0.05ps	0.02ps	0.01ps
25	E	1016.2	2076.4	3165	4445	5796.1	7120.4	8387.2
	τ	1.4ps	0.47ps	14.4 ps	0.16ps	0.04ps	0.02ps	0.01ps
30	E	1452	2495.9	3580.5	4862.7	6214.6	7525.1	8795.4
	τ	1.4ps	0.51ps	7.04ps	0.15ps	0.04ps	0.02ps	0.01ps

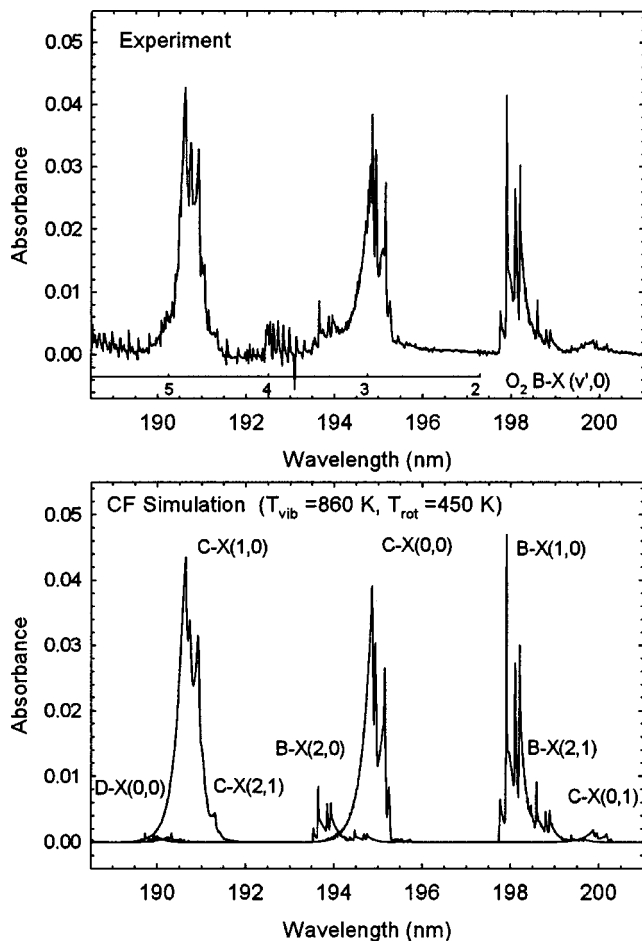


FIG. 3. Upper panel: Experimental absorption spectrum of the CF radical between 188.5 and 201 nm at a resolution of 0.02 nm in a C_4F_8/Ar plasma at 160 mTorr. Lower panel: Spectral simulation including the CF $B^2\Delta-X^2\Pi$, $C^2\Sigma^+-X^2\Pi$, and $D^2\Pi-X^2\Pi$ bands. The rotational temperature is 450 K and the vibrational temperature is 860 K. The transition probabilities of the CF $C^2\Sigma^+-X^2\Pi$ and $D^2\Pi-X^2\Pi$ bands are from *ab initio* electronic transition and RKR wave functions. The CF $C^2\Sigma^+-X^2\Pi$ intensities are normalized to the CF $B^2\Delta-X^2\Pi(1,0)$ and $(0,0)$ bands. The simulation also includes broadening from predissociation in the $C^2\Sigma^+-X^2\Pi(0,0)$ and $(1,0)$ bands. The location of the O_2 $B-X$ bandheads is also indicated. The role of O_2 interference in the lamp spectrum is discussed in the text.

cently, we have observed¹⁶ the very broadened CF $A-X(3,0)$ band [~ 16 cm^{-1} full width at half maximum (FWHM)] at 210 nm. This band was omitted in White's study also.

The lower panel of Fig. 3 displays the simulation of the CF spectra. There are three plots overlaid, corresponding to the CF $B-X$, $C-X$, and $D-X$ transitions. The hot bands are overlapped with the main bands for each system, as can be seen, for example, at 198.5 nm with the $B-X(1,0)$ and $B-X(2,1)$ bands. The simulation uses calculated absolute transition probabilities. Vibrational temperatures, rotational temperatures, and ground electronic state CF number density were determined from the well-characterized CF $A-X$ and $B-X$ bands¹⁷ in the same plasma conditions. From the $A-X$ bands the rotational temperature was determined to be 460 ± 20 K, and the vibrational temperature was 840 ± 40 K. The CF column density was 3.8×10^{14} cm^{-2} , which corresponds to a reactor center number density of

$(1.7 \pm 0.2) \times 10^{13}$ cm^{-3} after Abel inversion. The accuracy of these temperatures was confirmed by the good agreement between the observed and simulated $B-X(1,0)$ band shape, and by the ratio of the $B-X(1,0)$ and $(2,1)$ band intensities. The quality of the fits is similar for the $B-X$ and $C-X$ bands.

The resolution in the simulation was varied to obtain the best fit. The $B-X$ bands fit well with the instrumental resolution of 0.02 nm. The $C-X(0,0)$ band is best simulated with a Gaussian line shape with bandwidth of 0.035 nm (FWHM). Finally, the $C-X(1,0)$ is best fitted with a Lorentzian line shape with a bandwidth of 0.06 nm (FWHM). The $P_2 + Q_{12}$ bandhead of the $C-X(1,0)$ band is wider than the same bandhead for $C-X(0,0)$. The CF B $v'=0,1$ levels are known not to be predissociated, so the linewidths correspond to the instrumental resolution. Deconvolution of the broadening in the $C-X(0,0)$ and $(1,0)$ bands gives average broadenings of 4 ± 1 and 10 ± 2 cm^{-1} respectively, confirming that these bands cannot be rotationally resolved.

We found that the $C^2\Sigma^+ v'=0$ band is best fitted with a rotational constant $B_{v'=0} = 1.605 \pm 0.01$ cm^{-1} , in good agreement with White's¹⁴ value of $B_{v'=0} = 1.595 \pm 0.007$ cm^{-1} . For CF $C^2\Sigma^+ v'=1$, the interference from the O_2 bands in the lamp spectrum with the $C-X(1,0)$ is strong and the value of $B_{v'=1} \sim 1.56$ cm^{-1} is only an estimate. The vibrational spacing $\Delta G_{1,0}$ is 1135 ± 5 cm^{-1} , with part of the error arising from the uncertainty in the rotational constant. Table I summarizes the values of the energy terms, rotational constants, and predissociation lifetimes derived from the experimental data. We have included the data from White (attributed by him to $C'^2\Sigma^+ v'=0$ but labeled here as $C^2\Sigma^+ v'=2$) for comparison.

The *ab initio* calculations reproduce the $\Delta G_{1,0}$ spacing to within 25 cm^{-1} and the $\Delta G_{2,1}$ spacing to within 90 cm^{-1} . The predicted rotational constants are only 3% systematically smaller than the measured ones. The difference between the *ab initio* rotational constants, $(B_{v'=2} - B_{v'=0})$, is nearly identical to that observed experimentally.

The predissociation lifetimes for $v'=0$ and 1 are predicted within the error limits of the present experimental results. The $C^2\Sigma^+ v'=2$ appears to have a calculated predissociation lifetime that is too long, although the experimental result shows an unexpected increase of the predissociation lifetime compared to that of the $C^2\Sigma^+ v'=0$ and $v'=1$ levels. The calculations predict this qualitative behavior. White's thesis¹⁴ describes the predissociation of $C'^2\Sigma^+ v'=0$ as being rotationally dependent, increasing from at least 0.15 cm^{-1} at low rotational numbers to >1 cm^{-1} for $J=35.5$. Table III shows that the calculated predissociation rates increase very quickly with rotation, as is observed experimentally. Above the $C^2\Sigma^+ v'=2$ level, where there is no experimental data available, the calculations predict highly predissociated levels with nearly constant vibrational spacings because of the extensive perturbation. In summary, the *ab initio* calculations confirm the attribution of the peak at 190.7 nm to the $C-X(1,0)$ transition, and suggest very strongly that the previously designated $C'^2\Sigma^+ v'=0$ level, which had not been assigned to any known state, is in reality the $C^2\Sigma^+ v'=2$ level.

TABLE IV. Calculated vibrational transition probabilities for the CF $C^2\Sigma^+ - X^2\Pi(3-0, v'')$ with the *ab initio* electronic transition moment normalized to the CF $B^2\Delta - X^2\Pi(0,0)$ and (1,0) bands and RKR vibrational wave functions.

CF C-X					CF C-X						
band ($v'v''$)	$q_{v'v''}$	$r_{v'v''}$ (Å)	$\lambda_{v'v''}$ (Å)	$f_{v'v''}$	$A_{v'v''}$ (s^{-1})	band ($v'v''$)	$q_{v'v''}$	$r_{v'v''}$ (Å)	$\lambda_{v'v''}$ (Å)	$f_{v'v''}$	$A_{v'v''}$ (s^{-1})
0, 0	0.442 47	1.243	1950	1.25E-02	4.40E+07	1, 0	0.453 33	1.289	1908	1.64E-02	6.00E+07
0, 1	0.270 31	1.190	2000	5.68E-03	1.89E+07	1, 1	0.024 14	1.325	1956	1.31E-03	4.56E+06
0, 2	0.144 02	1.160	2052	2.80E-03	8.87E+06	1, 2	0.122 22	1.197	2006	2.85E-03	9.47E+06
0, 3	0.072 73	1.137	2106	1.42E-03	4.26E+06	1, 3	0.136 07	1.163	2057	2.75E-03	8.68E+06
0, 4	0.036 10	1.119	2162	7.27E-04	2.08E+06	1, 4	0.103 34	1.138	2110	2.04E-03	6.13E+06
0, 5	0.017 70	1.103	2220	3.73E-04	1.01E+06	1, 5	0.068 01	1.119	2165	1.39E-03	3.94E+06
0, 6	0.008 61	1.088	2280	1.91E-04	4.91E+05	1, 6	0.041 09	1.103	2222	8.74E-04	2.36E+06
0, 7	0.004 16	1.075	2342	9.78E-05	2.38E+05	1, 7	0.023 64	1.088	2281	5.29E-04	1.36E+06
						1, 8	0.013 15	1.075	2342	3.10E-04	7.54E+05
						1, 9	0.007 12	1.063	2406	1.77E-04	4.08E+05
						1,10	0.003 78	1.051	2471	9.91E-05	2.16E+05
2, 0	0.101 63	1.369	1866	5.86E-03	2.24E+07	3, 0	0.002 27	1.655	1830	4.80E-04	1.91E+06
2, 1	0.474 51	1.301	1912	1.91E-02	6.97E+07	3, 1	0.223 99	1.376	1874	1.34E-02	5.09E+07
2, 2	0.013 63	1.071	1960	3.39E-05	1.18E+05	3, 2	0.388 93	1.322	1920	1.81E-02	6.54E+07
2, 3	0.021 23	1.216	2010	6.48E-04	2.14E+06	3, 3	0.050 10	1.125	1967	5.00E-04	1.72E+06
2, 4	0.074 85	1.172	2060	1.63E-03	5.12E+06	3, 4	0.000 34	1.121	2015	1.41E-06	4.62E+03
2, 5	0.087 07	1.139	2112	1.76E-03	5.26E+06	3, 5	0.028 39	1.200	2066	7.29E-04	2.28E+06
2, 6	0.076 16	1.121	2166	1.57E-03	4.46E+06	3, 6	0.053 32	1.137	2117	1.11E-03	3.30E+06
2, 7	0.056 13	1.103	2223	1.21E-03	3.25E+06	3, 7	0.063 98	1.123	2171	1.33E-03	3.77E+06
2, 8	0.037 61	1.088	2281	8.44E-04	2.16E+06	3, 8	0.057 75	1.105	2226	1.26E-03	3.40E+06
2, 9	0.023 78	1.076	2341	5.63E-04	1.37E+06	3, 9	0.044 88	1.090	2284	1.02E-03	2.60E+06
2,10	0.014 41	1.064	2404	3.60E-04	8.30E+05	3,10	0.031 58	1.075	2343	7.49E-04	1.82E+06
2,11	0.008 40	1.053	2469	2.21E-04	4.83E+05	3,11	0.021 11	1.064	2405	5.27E-04	1.22E+06
2,12	0.004 76	1.041	2535	1.31E-04	2.71E+05	3,12	0.013 55	1.054	2469	3.57E-04	7.88E+05
2,13	0.002 65	1.030	2606	7.64E-05	1.50E+05	3,13	0.008 33	1.043	2535	2.30E-04	4.78E+05
						3,14	0.004 92	1.031	2604	1.42E-04	2.79E+05
						3,15	0.002 84	1.019	2675	8.50E-05	1.59E+05
						3,16	0.001 63	1.011	2749	5.09E-05	8.99E+04

C. CF $C^2\Sigma^+ - X^2\Pi$ and $D^2\Pi - X^2\Pi$ absolute transition probabilities

The $C^2\Sigma^+ - X^2\Pi$ and $D^2\Pi - X^2\Pi$ transition probabilities used in the simulation and displayed in Tables IV and V were obtained from the *ab initio* electronic transition moments and Rydberg–Klein–Rees (RKR) wave functions. The oscillator strength is defined by²⁰

$$f_{v'v''} = \frac{3.0376 \times 10^{-6}}{\lambda_{v'v''}} \cdot \frac{(2 - \delta_{0,\Lambda'+\Lambda''})}{(2 - \delta_{0,\Lambda''})} \times \left[\int \psi_{v'}(r) \cdot R_e(r) \cdot \psi_{v''}(r) dr \right]^2, \quad (3)$$

where ψ_v represent the vibrational wave functions, $R_e(R)$ is the electronic transition moment, λ is the wavelength of the transition (in cm), and δ_{ij} is the Kronecker delta, which is equal to 0 when $i \neq j$, and 1 when $i = j$. $\Lambda = 0$ for Σ states, and $\Lambda \neq 0$ for all the other states.

The related emission quantity, the vibrational Einstein emission coefficient between two levels $v'v''$ is, in units of s^{-1} :

$$A_{v'v''} = \frac{2.026 \times 10^{-6}}{\lambda_{v'v''}^3} \cdot \frac{(2 - \delta_{0,\Lambda'+\Lambda''})}{(2 - \delta_{0,\Lambda'})} \times \left[\int \psi_{v'}(r) \cdot R_e(r) \cdot \psi_{v''}(r) dr \right]^2. \quad (4)$$

Transition probabilities are calculated from the overlap of the vibrational wave functions. These are calculated from the potential energy curves by numerical integration of the Schrödinger equation. The potential energy curves can be obtained either from the *ab initio* calculations or by inverting the experimental vibrational and rotational molecular constants. The latter is the preferred method for diatomic molecules. The most common approach to calculate state potential curves from spectroscopic constants is the RKR method. In this work, we have used a computer program²¹ based on the algorithm described by Vanderslice.²² The RKR protocol implemented in the present work has been proven robust in other studies, most recently for the NO $A^2\Sigma^+ - X^2\Pi$ and $D^2\Pi - X^2\Pi$ electronic transitions.²³

In Table VI there is a complete list of the spectroscopic constants entered in the RKR calculations. The ground state constants have been determined in several studies.^{12,24,25} The most recent by Wollbrandt *et al.*¹² includes vibrational levels up to $v'' = 12$. Wollbrandt *et al.* also determined the $D^2\Pi$ state constants up to $v' = 6$ in the same experiment. That data set is more complete than previous determinations by Johnson *et al.*¹⁰ and Robberg *et al.*¹¹ The $C^2\Sigma^+$ state is problematic because of the extensive perturbations. We have chosen to use approximate molecular constants to represent the vibrational levels up to $v' = 2$.

Normalization of the CF C-X transition probabilities is

TABLE V. Calculated vibrational transition probabilities for the CF $D^2\Pi-X^2\Pi(0-3,v'')$ bands with the *ab initio* electronic transition moment and RKR vibrational wave functions.

CF $D-X$						CF $D-X$					
band ($v'v''$)	$q_{v'v''}$	$r_{v'v''}$ (Å)	$\lambda_{v'v''}$ (Å)	$f_{v'v''}$	$A_{v'v''}$ (s^{-1})	band ($v'v''$)	$q_{v'v''}$	$r_{v'v''}$ (Å)	$\lambda_{v'v''}$ (Å)	$f_{v'v''}$	$A_{v'v''}$ (s^{-1})
0, 0	0.084 43	1.211	1904	$3.71E-04$	$6.83E+05$	1, 0	0.236 29	1.240	1842	$1.04E-03$	$2.05E+06$
0, 1	0.178 98	1.191	1952	$7.84E-04$	$1.37E+06$	1, 1	0.180 16	1.217	1886	$7.97E-04$	$1.50E+06$
0, 2	0.212 49	1.171	2001	$9.24E-04$	$1.54E+06$	1, 2	0.034 81	1.194	1933	$1.56E-04$	$2.79E+05$
0, 3	0.187 20	1.153	2053	$8.05E-04$	$1.28E+06$	1, 3	0.003 32	1.194	1980	$1.34E-05$	$2.28E+04$
0, 4	0.137 03	1.135	2105	$5.81E-04$	$8.75E+05$	1, 4	0.052 52	1.164	2029	$2.23E-04$	$3.61E+05$
0, 5	0.088 44	1.118	2160	$3.68E-04$	$5.26E+05$	1, 5	0.099 37	1.145	2080	$4.19E-04$	$6.47E+05$
0, 6	0.052 18	1.103	2217	$2.12E-04$	$2.88E+05$	1, 6	0.111 46	1.128	2133	$4.64E-04$	$6.81E+05$
0, 7	0.028 86	1.088	2276	$1.14E-04$	$1.47E+05$	1, 7	0.096 50	1.112	2187	$3.94E-04$	$5.50E+05$
0, 8	0.015 22	1.073	2337	$5.82E-05$	$7.11E+04$	1, 8	0.071 32	1.096	2244	$2.84E-04$	$3.77E+05$
0, 9	0.007 74	1.059	2400	$2.85E-05$	$3.30E+04$	1, 9	0.047 40	1.082	2302	$1.84E-04$	$2.31E+05$
0,10	0.003 84	1.046	2466	$1.36E-05$	$1.49E+04$	1,10	0.029 23	1.068	2362	$1.10E-04$	$1.31E+05$
						1,11	0.017 07	1.055	2425	$6.16E-05$	$6.99E+04$
						1,12	0.009 57	1.042	2490	$3.31E-05$	$3.57E+04$
						1,13	0.005 21	1.03	2557	$1.72E-05$	$1.76E+04$
2, 0	0.297 02	1.270	1784	$1.31E-03$	$2.75E+06$	3, 0	0.222 26	1.302	1731	$9.77E-04$	$2.18E+06$
2, 1	0.014 39	1.239	1826	$6.36E-05$	$1.27E+05$	3, 1	0.059 29	1.283	1770	$2.64E-04$	$5.62E+05$
2, 2	0.061 70	1.229	1869	$2.71E-04$	$5.17E+05$	3, 2	0.129 48	1.254	1811	$5.71E-04$	$1.16E+06$
2, 3	0.119 83	1.206	1914	$5.28E-04$	$9.62E+05$	3, 3	0.007 06	1.222	1853	$3.17E-05$	$6.16E+04$
2, 4	0.057 69	1.184	1960	$2.56E-04$	$4.45E+05$	3, 4	0.037 17	1.219	1896	$1.62E-04$	$3.00E+05$
2, 5	0.003 40	1.153	2007	$1.63E-05$	$2.69E+04$	3, 5	0.087 83	1.196	1940	$3.85E-04$	$6.83E+05$
2, 6	0.011 80	1.160	2056	$4.77E-05$	$7.54E+04$	3, 6	0.057 34	1.174	1986	$2.53E-04$	$4.29E+05$
2, 7	0.049 12	1.138	2106	$2.02E-04$	$3.04E+05$	3, 7	0.010 53	1.151	2033	$4.82E-05$	$7.79E+04$
2, 8	0.076 69	1.121	2159	$3.13E-04$	$4.48E+05$	3, 8	0.001 82	1.165	2081	$6.49E-06$	$1.00E+04$
2, 9	0.082 33	1.105	2213	$3.30E-04$	$4.50E+05$	3, 9	0.024 50	1.133	2131	$9.80E-05$	$1.44E+05$
2,10	0.071 80	1.091	2268	$2.81E-04$	$3.64E+05$	3,10	0.051 23	1.115	2183	$2.05E-04$	$2.87E+05$
2,11	0.054 78	1.077	2326	$2.08E-04$	$2.57E+05$	3,11	0.065 37	1.100	2236	$2.57E-04$	$3.43E+05$
2,12	0.038 12	1.063	2386	$1.40E-04$	$1.64E+05$	3,12	0.064 95	1.086	2291	$2.49E-04$	$3.17E+05$
2,13	0.024 80	1.051	2447	$8.78E-05$	$9.78E+04$	3,13	0.055 28	1.072	2348	$2.06E-04$	$2.50E+05$
2,14	0.015 35	1.038	2512	$5.12E-05$	$5.51E+04$	3,14	0.042 36	1.059	2407	$1.53E-04$	$1.76E+05$
2,15	0.009 15	1.027	2578	$2.97E-05$	$2.98E+04$	3,15	0.030 10	1.047	2468	$1.05E-04$	$1.15E+05$
2,16	0.005 30	1.016	2647	$1.63E-05$	$1.56E+04$	3,16	0.020 21	1.035	2531	$6.74E-05$	$7.02E+04$
						3,17	0.013 00	1.024	2596	$4.14E-05$	$4.10E+04$
						3,18	0.008 08	1.013	2664	$2.45E-05$	$2.31E+04$

based on the CF $B-X(1,0)$ and $(0,0)$ bands; their oscillator strengths were optimized in a previous study.¹⁷ To obtain the agreement with the experimentally observed $C-X$ to $B-X$ band intensity ratio, we have incremented the calculated $C-X$ transition moment by 25%. The $D-X$ bands have not been optimized because of the lack of experimental data to compare with. The results suggest that the oscillator strength ratio of $f_{C-X(1,0)}/f_{D-X(0,0)}$ is ~ 40 .

In spite of the $C^2\Sigma^+$ state being perturbed, the experimental transition strengths in Fig. 3 are reproduced fairly

TABLE VI. RKR input spectroscopic constants (in cm^{-1}) for the states CF $X^2\Pi$, $C^2\Sigma^+$, and $D^2\Pi$ states.

Spectroscopic constant	CF $X^2\Pi$ (Ref. 12)	CF $C^2\Sigma^+$ (this work)	CF $D^2\Pi$ (Ref. 12)
$Y_{10} = \omega_e$	1307.93	1130	1807.44
$Y_{20} = -\omega_e x_e$	-11.08		-13.77
$Y_{30} = \omega_e y_e$	0.093		0.024
$Y_{40} = \omega_e z_e$	-0.001 08		
$Y_{01} = B_e$	1.416 26	1.615	1.730 01
$Y_{11} = -\alpha_e$	-0.018 44	-0.030	-0.019 413
$Y_{21} = \gamma_e$	0.000 122		0.000 054

accurately for the low vibrational levels in the spectra. The ratios $C-X(1,0)/C-X(2,1)$ and $C-X(0,0)/(0,1)$ at 840 K vibrational temperature are very close to the observed values. Also the ratio $C-X(1,0)/(0,0) \sim 1.3$ is well reproduced by the simulation. The ratio of the Franck-Condon factors for these two bands given in Table IV is about ~ 1 ; the improvement comes from the inclusion of the dependence of the electronic dipole moment on internuclear distance in the calculations.

The estimated oscillator strength for the $C-X(0,0)$ band is 0.0125 after normalization to the well characterized $B-X(0,0)$, $(1,0)$ and $A-X(2,0)$, $(1,0)$ bands. Adding the radiative cascading from the $C^2\Sigma^+$ state to the $A^2\Sigma^+$ state, calculated to be $\sim 10\%$ of the total emission ($f_{C-A(0,0)} \sim 0.11$), we obtain radiative lifetimes of 11 ± 2 and 9 ± 2 ns for the $C^2\Sigma^+$ $v'=0$ and $v'=1$ levels, compared with 18 and 15 ns from non-corrected *ab initio* calculations. According to the predissociation rates estimated from the observed spectral broadening, the fluorescence quantum yield of the $C^2\Sigma^+$ state in the absence of collisions is around 10^{-4} , explaining the lack of experimentally observed emission spectra from the CF $C-X$ bands.

The accuracy of the calculated transition probabilities

for the $C-X$ bands should decrease as the vibrational number increases because of the limited reliability of the spectroscopic constants of this perturbed state. Thus, we have not included vibrational levels higher than $C^2\Sigma^+ v'=3$ in the table. The $D-X$ transition probabilities suffer from a different problem. The vibrational wave functions have been well determined because the spectroscopic constants up to $v'=6$ are known, but the electronic transition moment has not been tested against experimental data, and the errors in the absolute transition probabilities can be up to 25%. It should be noted that the dependence on internuclear distance of *ab initio* transition moments are more reliable than their absolute values. Thus, the relative $D-X$ band strengths should be accurate. The $C^2\Sigma^+$ and $B^2\Delta$ states are too close to the $D^2\Pi$ state to cause a transition intensity of any importance. However, the $D-A$ transition is very strong ($f_{D-A(0,0)} \sim 0.7$) and accounts for $\sim 75\%$ of the total emission. The radiative lifetime of the $D^2\Pi v'=0$ state is estimated to be 35 ns. Predissociation may become important for the $^2\Pi^{(+)}$ levels¹⁶ and together with the strong $D-A$ transition in the infrared, makes the $D-X$ emission not a likely prominent feature of the CF spectra in the ultraviolet.

V. CONCLUSIONS

We have used a combination of new experimental data and *ab initio* calculations to characterize the irregular CF $C^2\Sigma^+ - X^2\Pi$ bands. We have observed a new band at 190.7 nm, and have assigned it to the CF $C^2\Sigma^+ - X^2\Pi$ (1,0) transition. The observed and calculated vibrational spacings, rotational constants, and predissociation rate variations show that the CF $C^2\Sigma^+$ Rydberg state is perturbed. We reassign the CF $C^2\Sigma^+ - X^2\Pi(0,0)$ and (0,1) bands as the CF

$C^2\Sigma^+ - X^2\Pi(2,0)$ and (2,1) bands. This reassignment solves long-standing inconsistencies in the interpretation of the CF radical UV spectra.

- ¹J. P. Booth, G. Hancock, and N. D. Perry, Appl. Phys. Lett. **50**, 318 (1987).
- ²T. Arai, M. Goto, K. Horikoshi, S. Mashino, and S. Aikyo, Jpn. J. Appl. Phys., Part 1 **38**, 4377 (1999).
- ³K. Miyata, M. Hori, and T. Goto, J. Vac. Sci. Technol. A **14**, 2343 (1996).
- ⁴S. Rauf and P. L. Ventzek, J. Vac. Sci. Technol. A **20**, 14 (2002).
- ⁵D. L'Esperance, B. A. Williams, and J. W. Fleming, Chem. Phys. Lett. **280**, 113 (1997).
- ⁶J. P. Booth, G. Cunge, L. Bienner, D. Romanini, and A. Kachanov, Chem. Phys. Lett. **317**, 631 (2000).
- ⁷J. P. Booth, Plasma Sources Sci. Technol. **8**, 249 (1999).
- ⁸G. A. Hebner, J. Appl. Phys. **89**, 900 (2001).
- ⁹C. Suzuki, K. Sasaki, and K. Kadota, J. Appl. Phys. **82**, 5321 (1997).
- ¹⁰R. D. Johnson and J. W. Hudgens, J. Phys. Chem. **91**, 6189 (1987).
- ¹¹M. Robberg, W. Strube, J. Wollbrandt, and E. Linke, J. Photochem. Photobiol., A **80**, 61 (1994).
- ¹²J. Wollbrandt, M. Rossberg, W. Strube, and E. Linke, J. Mol. Spectrosc. **176**, 385 (1996).
- ¹³W. P. White, R. M. Pitzer, C. W. Mathews, and T. H. Dunning, J. Mol. Spectrosc. **75**, 318 (1979).
- ¹⁴W. P. White, Ph.D. thesis, The Ohio State University, 1971.
- ¹⁵T. H. Dunning, J. Mol. Spectrosc. **75**, 297 (1979).
- ¹⁶I. D. Petsalakis, J. Chem. Phys. **110**, 10730 (1999).
- ¹⁷J. Luque, E. A. Hudson, and J. P. Booth, J. Chem. Phys. **118**, 622 (2003).
- ¹⁸J. Luque and D. R. Crosley, LIFBASE: Database and Spectral Simulation program 1.6 ed. (SRI International Report No. MP 99-009 (<http://www.sri.com/cem/lifbase>), 1999).
- ¹⁹G. W. Bethke, J. Chem. Phys. **31**, 669 (1959).
- ²⁰A. Schadee, J. Quant. Spectrosc. Radiat. Transf. **19**, 451 (1978).
- ²¹J. Ruiz and M. Martin, Comput. Chem. (Oxford) **19**, 417 (1995).
- ²²J. T. Vanderslice, E. A. Mason, W. G. Maisch, and E. R. Lippincott, J. Mol. Spectrosc. **3**, 17 (1959).
- ²³J. Luque and D. R. Crosley, J. Chem. Phys. **111**, 7405 (1999).
- ²⁴T. L. Porter, D. E. Mann, and N. Acquista, J. Mol. Spectrosc. **16**, 228 (1965).
- ²⁵M. A. Gondal, W. Rohrbach, W. Urban, R. Blanckart, and J. M. Brown, J. Mol. Spectrosc. **100**, 290 (1983).